Crystal structure and Hirshfeld surfaces analysis of Heterocyclic- and circulenes

Nataliya Karaush-Karmazin[1],* *Glib* Baryshnikov[1,2] , and *Boris* Minaev[1]

[1]Department of Chemistry and Nanomaterials Science, Bohdan Khmelnytsky National University, 18031 Cherkasy, Ukraine
[2]Linköping University, Department of Science and Technology, Laboratory of Organic Electronics, Norrköping, SE-60174 Sweden

Abstract. The crystal structure of the new diazatrioxa[9]circulene and tetrahydro-diazatetraoxa[10]circulene which represent the first synthesized representatives of "higher" hetero[n]circulenes with n>8, was analyzed in details. Hirshfeld surface analyses, the d_{norm} surfaces and two-dimensional fingerprint plots were used to verify the contributions of the different intermolecular interactions within the crystal structure of diazatrioxa[9]circulene and tetrahydro-diazatetraoxa[10]circulene. The Hirshfeld surface analysis of the crystal structure clarifies that the most important contribution for crystal packing is from H···H and C···H intermolecular interactions for both circulenes. The shape-index surface shows that in the case of diazatrioxa[9]circulene two sides of the molecules are involved with the same contacts in neighbouring molecules and curvedness plots show flat surface patches that are characteristic of planar stacking. Such face-to-face structural organization provides the main charge transfer pathway in [9]circulene. In the case of [10]circulene, the area involved in the same contacts is much less, however, two types of intermolecular packing modes can form such flat surface patches at curvedness plots which is useful for more efficient charge transfer.

Keywords: heterocirculenes, Hirshfeld surfaces analysis, Crystal structure.

1 Introduction

Heterocirculenes represent an important class of polyheterocyclic aromatic molecules because of their unique structural properties and promising application in optoelectronic devices, such as organic light-emitting diodes (OLEDs) [1–4] and organic field-effect transistors (OFETs) [5–7]. The molecules of hetero[n]circulenes consist of the central n-membered ring completely surrounded by and fused with benzene and heteroarene (furan, pyrrole, thiophene *etc*.) rings [8].

Until recently, the synthetic efforts of heterocyclic [n]circulenes covered up to eight aromatic rings (n = 8), while the higher hetero[n]circulenes (n>8) have been predicted only

* Corresponding author: karaush22@ukr.net

by quantum chemical modelling [9, 10]. Advances in the synthesis and quantum chemical simulations of heterocirculenes are summarized in reviews [11–14]. In 2020, the first synthesis of a fully aromatic [9]circulene, formally a diazatrioxa[9]circulene, along with a tetrahydro-diazatetraoxa[10]circulene was reported by the Pittelkow's group (Figure 1) [15].

The structural feature of heterocirculene molecules is their planar or quasi-planar structure responsible for the specific photophysical properties and unique architecture of their molecular crystals [16–19]. Remarkably, that the electronic properties of heterocirculene molecules can be easily tuned *via* diverse chemical modifications. In particular, the replacement of one heteroatom by another or the introduction of side substituents into the heterocirculene molecule significantly affect their electronic molecular structure and structural organization in the solid-state. The relationship between crystal packing and transport properties for a series of synthesized hetero[8]circulenes is highlighted in our recent paper [20].

In this paper, we have systematically studied the crystal structure of the novel diazatrioxa[9]circulene and tetrahydro-diazatetraoxa[10]circulene. The application of Hirshfeld surface analysis approach [21] represent a convenient tool for the investigation of intermolecular interactions in crystals. The analysis of the Hirschfeld surface is especially suitable for visualizing the variations in intermolecular interactions in compounds and is becoming more common in crystalography. Plotting the corresponding fingerprint plots [22] provides a quantitative analysis of all types of intermolecular contacts that are present in the molecule and presents this information on a color plot.

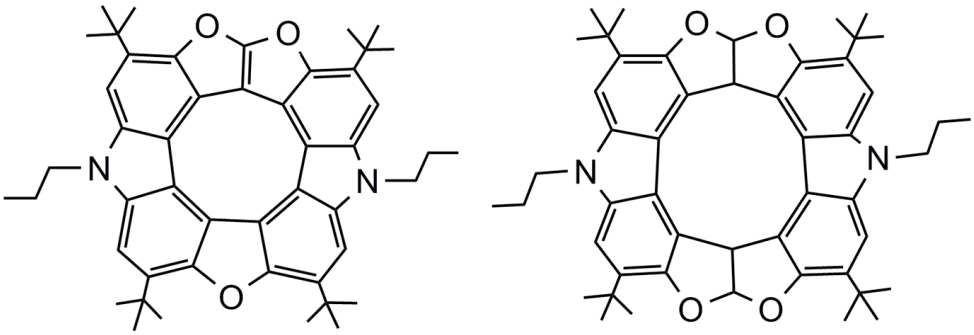

Fig. 1. Molecular structures of the studied heterocyclic [9]- and [10]circulenes.

2 Computational details

The Hirshfeld surface analysis represents a quantitative way to study the intermolecular interactions in crystalline systems. The Hirshfeld surfaces of the studied [9]- and [10]circulenes and its corresponding two-dimensional (2D) fingerprint plots were calculated with the aid of the Crystal Explorer 17.5 software at very high resolution [23–25]. The analysis is visualized by the normalized contact distance (d_{norm}), which is defined in terms of external and internal distances (d_e and d_i, respectively) and the van der Waals radii (*vdW*) of atoms and is computed with the following equation 1:

$$d_{norm} = \frac{d_i - r_i^{vdW}}{r_i^{vdW}} + \frac{d_e - r_e^{vdW}}{r_e^{vdW}} \quad (1)$$

where, r_i^{vdW} and r_e^{vdW} are the van der Waals radii of the appropriate atoms internal and external to the surface, respectively. The contacts with distances equal to the sum of the *vdW* radii are indicated in white and the contacts with distances shorter or longer than *vdW* radii are represented in red and blue, respectively.

3 Results and discussion

3.1 Structural analysis

The compound of diazatrioxa[9]circulene crystallizes in the orthorhombic system in space group *Pbca*; tetrahydro[10]circulene possesses triclinic crystalline structure of *P-1* symmetry space group (Figure 2). In crystal the structure of [9]circulene macrocyclic core is perfectly planar, however, the presence of *tert*-butyl and propyl groups prevents the formation of a layered structure that is characteristic of planar heterocirculenes [20]. In the case of [9]circulene, the molecules form zigzag-type ribbons along *ac* plane (Figure 2*a*).

The tetrahydro[10]circulene adopts V-shaped *cis* form with unilaterally directed hydrogen atoms on four bridging sp^3 carbon atoms. The angle between the mean-plane of the two carbazoles is 73.7°. V-shaped molecules are stacked in a crystal in such a way that one molecule provides a free vacancy for the *tert*-butyl and propyl groups of another molecule (Figure 2*b*).

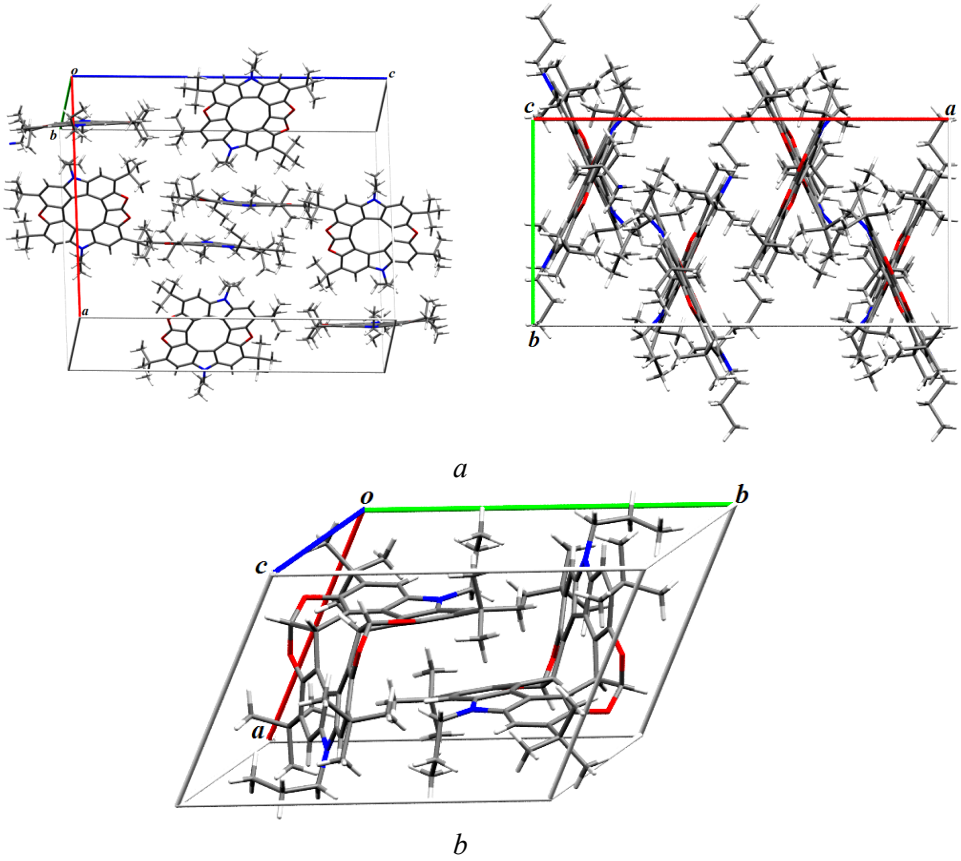

Fig. 2. Crystal structure of diazatrioxa[9]circulene and tetrahydro-diazatetraoxa[10]circulene.

3.2 Hirshfeld surface analysis

Hirshfeld surface analysis is performed in order to underpin the nature of the intermolecular contacts stabilizing the crystal structures of the diazatrioxa[9]circulene and tetrahydro-diazatetraoxa[10]circulene.

3.2.1. [9]Circulene

A Hirshfeld surface of diazatrioxa[9]circulene is illustrated in figure 3 and represents the interaction of the electron density of selected molecule with that of the surrounding crystal medium. Figure 3*a*, *b* shows that [9]circulene possesses two red spots, indicating contacts of hydrogen atom with each carbon atom of closely located benzene ring.

The shape-index map of the [9]circulene molecule was generated in the ranges −1 to 1 Å and is presented in figure 3*c*. From the shape-index map, it can be seen that the molecules are related to one another by π-π stacking interactions, which are indicated by adjacent red and blue triangles (highlighted by grey circles) on the shape-index surface. The blue triangles represent convex regions and symbolize the presence of ring carbon atoms of the molecule inside the surface, while the red triangles symbolize concave regions caused by carbon atoms of the π-stacked molecule above it. The presence of π-π stacking is clearly visible on the curvedness surface, generated in the ranges −4 to 4 Å (Figure 3*d*). The large green regions represent a relatively planar surface area, while the blue regions demonstrate areas of curvature. On the Hirshfeld surface the π–π stacking interactions is evident as planar green regions around the rings where the contact distances are similar (Figure 3*d*).

It should be noted that in the case of diazatrioxa[9]circulene the π-π stacks provides the main charge transfer pathway than other configurations with the hole and electron transfer integral for π-π stack modes are of 7.58 and 8.35 meV, respectively [15]. The final hole and electron mobility values in [9]circulene were reported to be 0.013 and 0.038 $cm^2\ V^{-1}\ s^{-1}$, respectively [15].

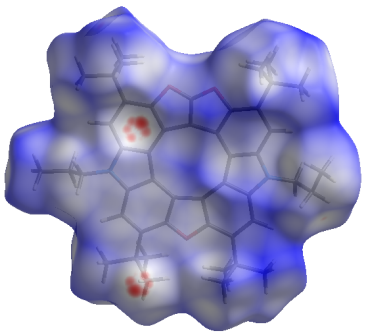

a

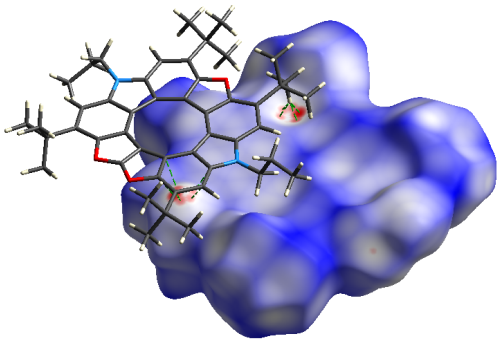

b

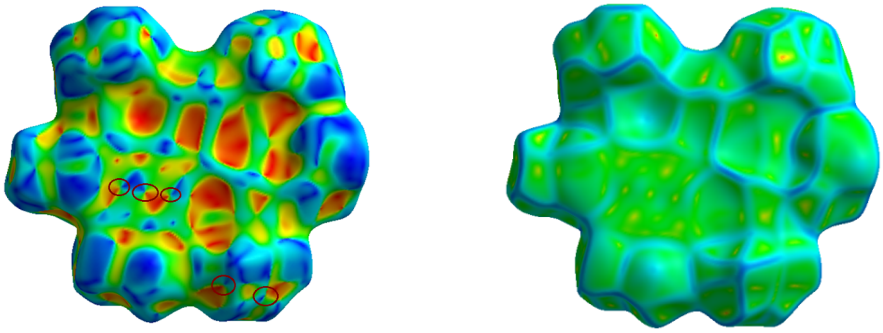

Fig. 3. Hirshfeld d_{norm} surface (*a* and *b*) of the intermolecular interactions, shape index map (*c*), and curvedness map (*d*) for diazatrioxa[9]circulene.

The two-dimensional (2D) fingerprint plot illustrates the contributions from the different intermolecular interaction types that overlap in the full fingerprint and then separated. The 2D fingerprint plot of [9]circulene is demonstrated in figure 4 and reveals that the main intermolecular interactions in [9]circulene are H···H, C···H, O···H and C···C contacts. For [9]circulene the shortest contacts correspond to the very close H···H contacts, showing a sharp spike centred near a (d_e+ d_i) sum of 2.0 Å. The decomposition of the fingerprint plot shows that H···H contacts occupy 66.9 % of the total Hirshfeld surface area, C···H contacts − 26.3 %, O···H and C···C contacts contribute only 4.0 % and 1.4 %, respectively, to the total Hirshfeld surface area.

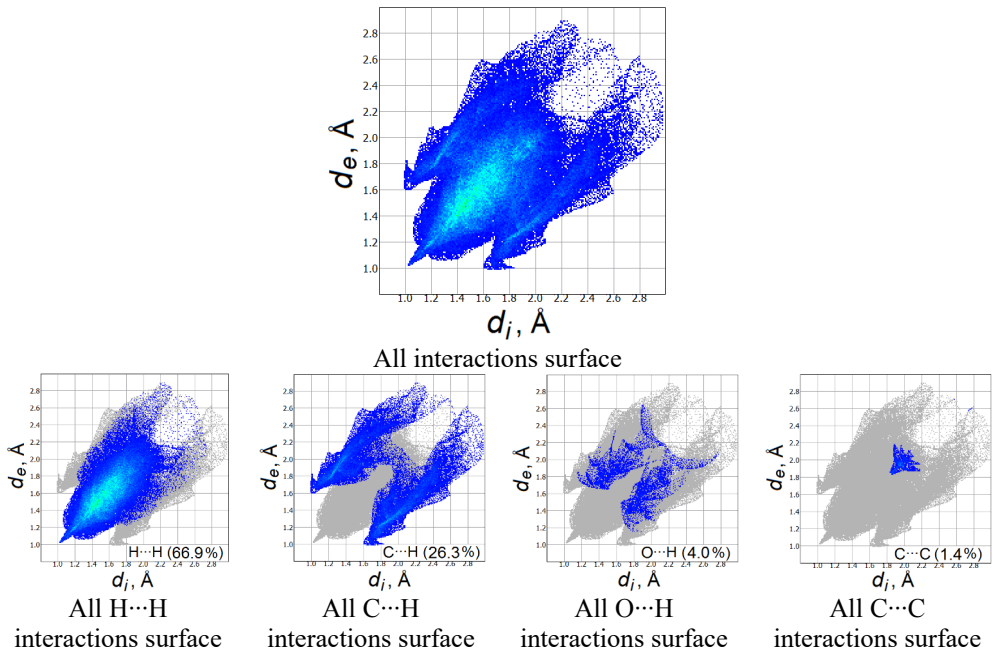

Fig. 4. Fingerprint plots for diazatrioxa[9]circulene (The d_e and d_i denote the external and internal distances, respectively). Below are presented the relative contributions of the intermolecular interactions to the Hirshfeld surface (%); interactions with contributions less than 1 % are not presented here.

3.2.2. [10]Circulene

The 3D representations of a Hirshfeld surface for tetrahydro[10]circulene is presented in figure 5. The distinct circular depressions (red spots) on the d_{norm} surface correspond to the short C···H contacts (Figure 5*a*). The presence of the adjacent red and blue triangles (highlighted by grey circles) on the shape-index surface (Figure 5*d*) indicates the two sides of the [10]circulene molecules are associated with the same contacts in neighboring molecules, and the curvature plot (Figure 5*e*) show flat surface areas that are characteristic of planar overlap. It is interesting to note, that in the case of [10]circulene, the packing modes in figures 5*a* and 5*b* provide the main pathways for charge transfer with final hole and electron mobility calculated to be 0.163 and 0.009 $cm^2 V^{-1} s^{-1}$, respectively [15].

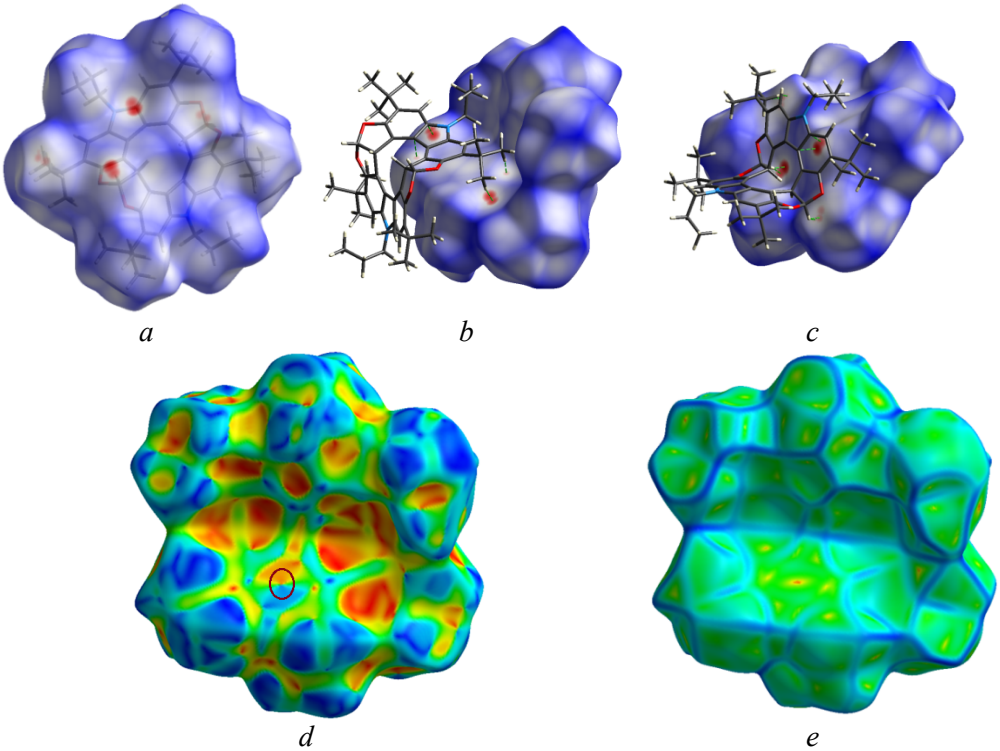

Fig. 5. Hirshfeld d_{norm} surface (*a*-*c*) of the intermolecular interactions, shape index map (*d*), and curvedness (*c*) for tetrahydro[10]circulene.

The relative contributions of the intermolecular contacts to the Hirshfeld surface area in tetrahydro[10]circulene crystal are shown in figure 6. For tetrahydro[10]circulene the H···H interactions have the main contribution (76.5%) to the total Hirshfeld surface. The C···H contacts contribute 18.6%, other intermolecular O···H and N···H contacts contribute only 2.9 % and 1.0 %, respectively, to the total Hirshfeld surface area.

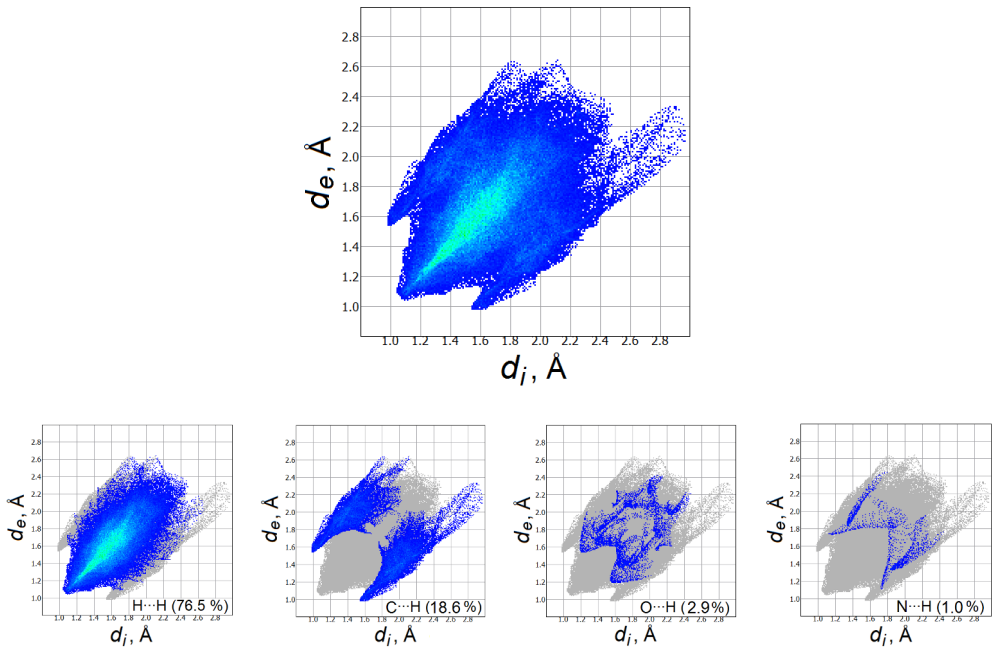

Fig. 6. Fingerprint plots for tetrahydro[10]circulene (The d_e and d_i denote the external and internal distances, respectively). Below are presented the relative contributions of the intermolecular interactions to the Hirshfeld surface (%); interactions with contributions less than 1 % are not presented here.

4 Conclusion

In this study, we have performed a detailed analysis of the X-ray crystals for both [9]- and [10]circulenes based on the Hirshfeld surface analysis and their associated two-dimensional fingerprint plots to provide a complete understanding of the intermolecular interactions in a facile and immediate way. Molecular Hirshfeld surfaces revealed that the [9]- and [10]circulene compounds were supported mainly by H···H and C···H intermolecular interactions. It was also shown that the [9]circulene possesses π-π stacking interactions that follows from the shape index and curvedness maps. Moreover, fingerprint plots made it possible to identify all types of intermolecular interactions present in [9]- and [10]circulene crystals.

There are no conflicts to declare.

This work was supported by the Ministry of Education and Science of Ukraine (Project 0121U107533).

References

1. Nielsen C B, Brock-Nannestad T, Reenberg T K, Hammershøj P, Christensen J B, Stouwdam J W and Pittelkow M 2010 *Chem. Eur. J.* vol 16 pp 13030–13034
2. Baryshnikov G V, Valiev R R, Karaush N N, Minaeva V A, Sinelnikov A N, Pedersen S K, Pittelkow M, Minaev B F and Ågren H 2016 *Phys. Chem. Chem. Phys.* vol 18 pp 28040–28051

3. Ivaniuk K B, Baryshnikov G V, Stakhira P Y, Pedersen S K, Pittelkow M, Lazauskas A, Volyniuk D, Grazulevicius J V, Minaev B F and Ågren H 2017 *J. Mater. Chem. C* vol 5 pp 4123–4128
4. Pedersen S K, Pedersen V B, Kamounah F S, Broløs L M, Baryshnikov G V, Valiev R R, Ivaniuk K, Stakhira P, Karaush-Karmazin N N, Minaev B, Ågren H and Pittelkow M 2021 Chem–A Eur J (In Press) doi.org/10.1002/chem.202100090
5. Fujimoto T, Matsushita M M and Awaga K 2012 *J. Phys. Chem. C* vol 116 pp 5240–5245
6. Fujimoto T, Matsushita M M and Awaga K, 2010 *Appl. Phys. Lett.* vol 97 pp 123303–123305
7. Dadvand A, Cicoira F, Chernichenko K Yu, Balenkova E S, Osuna R M, Rosei F, Nenajdenko V G and Perepichka D F 2008 *Chem. Commun.* pp 5354–5356
8. Dopper J H and Wynberg H 1972 Tetrahedron Lett. vol 13 pp 763–766
9. Karaush N N, Baryshnikov G V, Ågren H and Minaev B F 2018 *New J. Chem.* vol 42 pp 11493–11505.
10. Karaush-Karmazin N N, Baryshnikov G V, Valiulina L I, Valiev R, Ågren H and Minaev B 2019 *New J. Chem.* vol 43, pp 12178–12190
11. Baryshnikov G V, Minaev B F and Minaeva V A 2015 *Russ. Chem. Rev.* vol 84 pp 455–484
12. Hensel T, Andersen N N, Plesner M and Pittelkow M 2016 *Synlett.* pp 498–525
13. Karaush N N, Baryshnikov G V, Minaeva V A, Ågren H and Minaev B F 2017 *Mol. Phys.* vol 115 pp 2218–2230
14. Miyake Y and Shinokubo H 2020 *Chem. Commun.* vol 56 pp 15605–15614
15. Pedersen S K, Eriksen K, Ågren H, Minaev B F, Karaush-Karmazin N N, Hammerich O, Baryshnikov G V and Pittelkow M 2020 *J. Am. Chem. Soc.* vol 142, pp 14058–14063
16. Baryshnikov G V, Valiev R R, Cherepanov V N, Karaush-Karmazin N N, Minaeva V A, Minaev B F and Ågren H 2019 *Phys. Chem. Chem. Phys.* vol 21 pp 9246–9254
17. Ivasenko O, MacLeod J M, Chernichenko K Yu, Balenkova E S, Shpanchenko R V, Nenajdenko V G, Rosei F and Perepichka D F, 2009 *Chem. Commun.* pp. 1192–1194.
18. Kato S, Akahori S, Serizawa Y, Lin X, Yamauchi M, Yagai S, Sakurai T, Matsuda W, Seki S, Shinokubo H and Miyake Y 2020 *J. Org. Chem.* vol 85 pp 62–69
19. Akahori S, Sakai H, Hasobe T, Shinokubo H and Miyake Y 2018 *Org. Lett.* vol 20 pp 304–307
20. Karaush-Karmazin N N, Baryshnikov G V, Kuklin A V, Saykova D I, Ågren H and Minaev B 2021 *J. Mat. Chem. C* vol 9 pp 1451–1466
21. Seth S K, Saha I, Estarellas C, Frontera A, Kar T and Mukhopadhyay S 2011 *Cryst. Growth Des.* vol 11 pp. 3250–3265
22. Rohl A L, Moret M, Kaminsky W, Claborn K, Mckinnon J J and Kahr B 2008 *Cryst. Growth Des.* vol 8 pp. 4517–4525
23. Turner M J, McKinnon J J, Wolff S K, Grimwood D J, Spackman P R, Jayatilaka D and Spackman M A 2017 *Crystal Explorer 17.5* University of Western Australia, Perth.
24. Spackman M A and McKinnon J J 2002 *Crystengcomm* vol 4 pp 378–392
25. McKinnon J J, Spackman M A and Mitchell A S 2004 *Acta Crystallogr. Sect. B Struct. Sci.* vol 60 pp 627–668